ICSV 21
13-17 July, 2014, Beijing/China

The 21st International Congress on Sound and Vibration

13-17 July, 2014, Beijing/China

ACOUSTIC STATE-SPACE MODELS USING A WAVE-BASED APPROACH

Simon J. Illingworth

Department of Mechanical Engineering, University of Melbourne, VIC 3010, Australia
e-mail: sillingworth@unimelb.edu.au

Matthew P. Juniper

Department of Engineering, University of Cambridge, Cambridge CB2 1PZ, UK

A wave-based analysis is a convenient method for generating acoustic models, both for simple and for more complex geometries. However, there is no straightforward method to describe the resulting system in state-space form. This prevents powerful, well-established methods from dynamics and control being applied to a wave-based acoustic model because these methods require a state-space description of the system to which they are applied. This paper presents a simple method for generating a state-space description of an acoustic model when that model has been derived using a wave-based approach. The utility of the method is demonstrated by applying it to a simple open-ended duct with a temperature jump across the flame, and the resulting state-space model is validated in both the time domain and the frequency domain. The method is sufficiently general that it can also be applied to more complex geometries.

1. Introduction

There are a number of ways to formulate an acoustic model for a thermoacoustic analysis. Three common methods are i) a Galerkin discretization [1–3]; ii) a Green's function approach [4] (which may subsequently be used in a modal expansion [5]); and iii) a wave-based approach [6, 7]. In any acoustic modelling method, it is very useful if one can write the resulting model in state-space form (to be defined in § 4) because this description of the acoustics allows allows one to make use of powerful techniques from dynamics and control. This could include a stability analysis of the coupled thermoacoustic system; analysis of its transient growth characteristics; or feedback controller design to eliminate oscillations. For the first two methods mentioned above – namely the Galerkin discretization and the Green's function approach – methods to describe the resulting systems in state-space form have been developed. For a Galerkin discretization, a state-space description follows quite naturally from the Galerkin modes, and for a Green's function approach, a state-space description can be generated by performing a modal expansion [5]. For the wave-based approach, however, it is less straightforward to describe the resulting system in state-space form, and this is largely due to the explicit presence of time delay terms, which make the system infinite-dimensional, and which are not amenable to a state-space description in a straightforward way.

The purpose of this paper is to present a method for generating a state-space description of an acoustic model when that model has been derived using a wave-based analysis. The method is applied to a simple open-ended duct geometry with a temperature jump across the flame. However, the method is sufficiently general that it could equally well be applied to more complex geometries using data generated by a suitable low-order model, such as the time-domain network model described by Stow & Dowling [8]. The paper is organized as follows. In § 2 the wave-based acoustic analysis is described. In § 3 the simplifying assumption of no mean flow is made. This is done to make the model more tractable, allowing one to readily give physical significance to the different terms. In § 4 a method for generating a state-space description of the wave-based model is introduced, and in § 5, results of the approach applied to a simple geometry (with mean flow) are presented. We conclude the paper in § 6.

2. Wave-based approach for a duct with mean flow

Figure 1 shows the geometry considered: an acoustically compact flame sits in a duct of unity length. Steady heat release gives rise to a change in temperature across the flame (and therefore a change in the mean speed of sound from $\bar{c}_1$ before combustion to $\bar{c}_2$ after combustion). A perturbation in the heat release, $q'(t)$, generates outward-travelling waves that propagate both upstream (α_1) and downstream (α_2). These waves are reflected when they reach the upstream/downstream ends of the duct. This reflection is characterized by the reflection coefficients, R_1 and R_2, and gives rise to reflected waves β_1 and β_2. Notice that we have defined the spatial coordinate system, x, such that $x = 0$ at the flame. Then $x \in [-l_1, 0]$ upstream of the flame and $x \in [0, l_2]$ downstream of the flame.

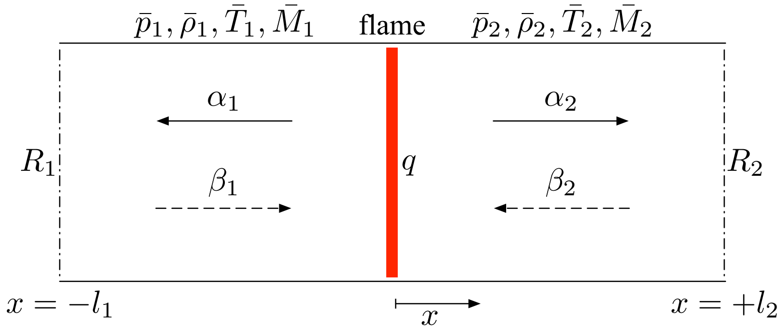

Figure 1. Wave approach in a simple duct geometry.

2.1 Wave approach

We solve the wave equation in each of the two regions upstream and downstream of the flame shown in figure 1. Considering the region upstream of the flame, the acoustic pressure and velocity perturbations can be written in terms of the upstream- and downstream-travelling waves, α_1 and β_1:

$$p_1'(x,t) = \alpha_1(t + \tfrac{x}{\bar{c}_1 - \bar{u}_1}) + \beta_1(t - \tfrac{x}{\bar{c}_1 + \bar{u}_1}) \tag{1a}$$

$$\rho_1'(x,t) = \frac{1}{\bar{c}_1^2}[\alpha_1(t + \tfrac{x}{\bar{c}_1 - \bar{u}_1}) + \beta_1(t - \tfrac{x}{\bar{c}_1 + \bar{u}_1})] \tag{1b}$$

$$u_1'(x,t) = \frac{1}{\bar{\rho}_1 \bar{c}_1}[-\alpha_1(t + \tfrac{x}{\bar{c}_1 - \bar{u}_1}) + \beta_1(t - \tfrac{x}{\bar{c}_1 + \bar{u}_1})]. \tag{1c}$$

We can write similar expressions for the downstream region [6].

2.2 Boundary conditions

Boundary conditions are required at the ends of the duct and across the flame. The boundary condition at the upstream end, $x = -l_1$, is:

$$\begin{aligned} \beta_1(t + \tfrac{l_1}{\bar{c}_1 + \bar{u}_1}) &= R_1 \alpha_1(t - \tfrac{l_1}{\bar{c}_1 - \bar{u}_1}) \\ \Rightarrow \beta_1(t) &= R_1 \alpha_1(t - \tau_1), \end{aligned} \tag{2}$$

where $\tau_1 = 2l_1\bar{c}_1/(\bar{c}_1^2 - \bar{u}_1^2)$. Similarly, at the downstream end, $x = l_2$, we have:

$$\begin{aligned} \beta_2(t + \tfrac{l_2}{\bar{c}_2 - \bar{u}_2}) &= R_2\alpha_2(t - \tfrac{l_2}{\bar{c}_2 + \bar{u}_2}) \\ \Rightarrow \beta_2(t) &= R_2\alpha_2(t - \tau_2), \end{aligned} \tag{3}$$

where $\tau_2 = 2l_2\bar{c}_2/(\bar{c}_2^2 - \bar{u}_2^2)$.

2.3 Momentum and energy equations

At the flame (where $x = 0$), Dowling [9] uses the two conditions:

$$p_2 - p_1 + \rho_1 u_1(u_2 - u_1) = 0 \tag{4a}$$

$$\frac{\gamma}{\gamma - 1}(p_2 u_2 - p_1 u_1) + \frac{1}{2}\rho_1 u_1(u_2^2 - u_1^2) = Q, \tag{4b}$$

where Q is the total heat release rate. Assuming the upstream mean flow is prescribed, then we have two unknowns, $\bar{u}_2$ and $\bar{p}_2$, and two equations. Solving them gives rise to two quadratic equations, which we can solve for $\bar{u}_2$ and $\bar{p}_2$. For linearized disturbances, Eq. (4) becomes:

$$p_2' - p_1' + \bar{\rho}_1\bar{u}_1(u_2' - u_1') + (\bar{u}_2 - \bar{u}_1)(\bar{\rho}_1 u_1' + \bar{u}_1\rho_1') = 0 \tag{5a}$$

$$\frac{\gamma}{\gamma - 1}(\bar{p}_2 u_2' + \bar{u}_2 p_2' - \bar{p}_1 u_1' - \bar{u}_1 p_1') + \bar{\rho}_1\bar{u}_1(\bar{u}_2 u_2' - \bar{u}_1 u_1') + \frac{1}{2}(\bar{u}_2^2 - \bar{u}_1^2)(\bar{\rho}_1 u_1' + \bar{u}_1\rho_1') = q'. \tag{5b}$$

2.4 Solution for waves

Substituting the expressions for the perturbation quantities (Eq. 1) into the linearized equations (Eq. 5) and recalling that they apply at the flame where $x = 0$, we arrive at two equations for the wave amplitudes, which we write in matrix form as

$$X\begin{bmatrix}\alpha_1(t)\\ \alpha_2(t)\end{bmatrix} - Y\begin{bmatrix}\beta_1(t)\\ \beta_2(t)\end{bmatrix} = \begin{bmatrix}0\\ 1\end{bmatrix}\frac{q'(t)}{\bar{c}_1}, \tag{6}$$

where X and Y are 2×2 matrices, the expressions for which are given in Appendix A. At this point we have two equations but four unknowns. By using the boundary conditions at the duct ends, we arrive at the requisite two unknowns, which gives an equation governing the time evolution of the outward-travelling waves $\alpha_1(t), \alpha_2(t)$:

$$X\begin{bmatrix}\alpha_1(t)\\ \alpha_2(t)\end{bmatrix} = Y\begin{bmatrix}R_1\alpha_1(t - \tau_1)\\ R_2\alpha_2(t - \tau_2)\end{bmatrix} + \begin{bmatrix}0\\ 1\end{bmatrix}\frac{q'(t)}{\bar{c}_1}, \tag{7}$$

Taking Laplace transforms, the resulting system can be written as

$$\begin{bmatrix}X_{11} - R_1Y_{11}e^{-s\tau_1} & X_{12} - R_2Y_{12}e^{-s\tau_2}\\ X_{21} - R_1Y_{21}e^{-s\tau_1} & X_{22} - R_2Y_{22}e^{-s\tau_2}\end{bmatrix}\begin{bmatrix}\alpha_1(s)\\ \alpha_2(s)\end{bmatrix} = \begin{bmatrix}0\\ 1\end{bmatrix}\frac{q(s)}{c_1}. \tag{8}$$

The modes of the system are then given by those values of s where the determinant of Eq. (8) vanishes. We can now solve for α_1 and α_2 by rearranging Eq. (8):

$$\alpha_1(s) = -\tfrac{1}{\bar{c}_1}(X_{12} - Y_{12}R_2e^{-s\tau_2})q(s)/\Omega(s) \tag{9a}$$

$$\alpha_2(s) = +\tfrac{1}{\bar{c}_1}(X_{11} - Y_{11}R_1e^{-s\tau_1})q(s)/\Omega(s), \tag{9b}$$

where $\Omega(s)$ is the determinant of the matrix in Eq. (8).

2.5 Solution for pressure and velocity perturbations

We can now substitute these expressions into Eq. (1) to find expressions for the pressure and velocity for the upstream region:

$$\frac{p_1'(x,s)}{q'(s)} = -\frac{[X_{12} - R_2 Y_{12} e^{-s\tau_2^{2l}}][+1 + R_1 e^{-s\tau_1^{2(l-x)}}]}{\bar{c}_1 \Omega(s)} e^{-s\tau_1^x} \tag{10a}$$

$$\frac{u_1'(x,s)}{q'(s)} = -\frac{[X_{12} - R_2 Y_{12} e^{-s\tau_2^{2l}}][-1 + R_1 e^{-s\tau_1^{2(l-x)}}]}{\bar{\rho}_1 \bar{c}_1^2 \Omega(s)} e^{-s\tau_1^x}. \tag{10b}$$

A similar analysis can be performed for the downstream region.

3. Waved-based approach without mean flow

In this section we look at what happens when we neglect the mean flow. By doing so the expressions just derived simplify significantly, and we use them to give some physical significance to the different terms. For no mean flow, Eq. (8) simplifies to

$$\begin{bmatrix} 1 + R_1 e^{-s\tau_1} & -1 - R_2 e^{-s\tau_2} \\ 1 - R_1 e^{-s\tau_1} & \frac{c_2}{c_1}(1 - R_2 e^{-s\tau_2}) \end{bmatrix} \begin{bmatrix} \alpha_1(s) \\ \alpha_2(s) \end{bmatrix} = \begin{bmatrix} 0 \\ \frac{\gamma-1}{c_1} \end{bmatrix} q(s), \tag{11}$$

and the modes occur at values of s satisfying

$$\frac{c_2}{c_1}(1 + R_1 e^{-s\tau_1})(1 - R_2 e^{-s\tau_2}) + (1 - R_1 e^{-s\tau_1})(1 + R_2 e^{-s\tau_2}) = 0. \tag{12}$$

It is convenient to write this as

$$(1 + \frac{c_2}{c_1})(1 - R_1 R_2 e^{-s(\tau_1+\tau_2)}) + (1 - \frac{c_2}{c_1})(R_2 e^{-s\tau_2} - R_1 e^{-s\tau_1}) = 0. \tag{13}$$

This is convenient because it makes clear the influence of c_2/c_1. When $c_2/c_1 = 1$ (no temperature change across the flame), the modes are equispaced and given simply by

$$R_1 R_2 e^{-s(\tau_1+\tau_2)} = 1. \tag{14}$$

When $c_2/c_1 \neq 1$ we have an extra term in Eq. (13) and the modes are no longer equispaced. We can now use Eq. (8) to ultimately solve for the pressure and velocity as we did before. For the upstream region the solution is

$$p_1(x_1,s) = \frac{\gamma-1}{c_1} \frac{[1 + R_2 e^{-s\tau_2}][1 + R_1 e^{-s(\tau_1 - \frac{2x_1}{c_1})}]}{\Omega(s)} e^{-s\frac{x_1}{c_1}} q(s) \tag{15a}$$

$$u_1(x_1,s) = \frac{\gamma-1}{2\rho_1 c_1^2} \frac{[1 + R_2 e^{-s\tau_2}][-1 + R_1 e^{-s(\tau_1 - \frac{2x_1}{c_1})}]}{\Omega(s)} e^{-s\frac{x_1}{c_1}} q(s). \tag{15b}$$

We now consider what the terms in each of the numerators represent.

- $1 + R_2 e^{-s\tau_2}$ term: this appears in both the pressure and the velocity, and that is because it comes from the expression for $\alpha_1(s)$ in Eq. (9a). It tells us that we will have zero response (an antiresonance) whenever $1 + R_2 e^{-s\tau_2} = 0$. Physically, what do the two terms represent? Imagine that acoustic perturbations are zero everywhere in the duct. A fluctuation in q will then generate two waves directly: α_1 and α_2. The 1 in the expression is just the α_1 wave generated directly by q. The $R_2 e^{-s\tau_2}$ is the α_2 wave which, after reflecting from the downstream boundary, arrives back at the flame and is 'turned into' an α_1 wave as it traverses the flame – i.e. it is the 'echo' of the α_2 wave. From these arguments we see that these zeros have nothing to do with where one measures p_1 or u_1. They are completely determined by the location of the flame in the duct.

- $\pm 1 + R_1 e^{-s(\tau_1 - \frac{2x_1}{c_1})}$ term: this is another source of zeros. It depends on both frequency, s and the location, x_1, and so where we measure is important this time. Physically, these zeros occur when the wave α_1 and its reflection β_1 cancel each other out.

To summarize (for region 1 of the duct): The first source of zeros occurs when the wave α_1 generated by q is exactly cancelled by the reflection of the wave α_2 from the other side of the duct. In this sense q is not able to excite α_1 at this particular s, and if α_1 is zero, then p_1 and u_1 are zero everywhere. The second source of zeros occurs when, although α_1 is excited, it is cancelled out by its own reflection, β_1. We can perform the same analysis for the other half of the duct, and similar physical significance can be given to the different terms.

4. Finding a state-space model

Having outlined the wave-based approach for finding an acoustic model, we now look at how one can use knowledge of the acoustic modes, together with knowledge of the frequency response, to find a state-space description of such a model.

4.1 Finding modes

Rather than discretize the system using some kind of discretization scheme (such as Galerkin modes), we will discretize the system by finding its eigenvalues directly. This involves finding the roots, $\lambda_j = \sigma_j + i\omega_j$, of $\Omega(s)$ introduced in § 2.4:

$$\Omega(s) = (X_{11} - R_1 Y_{11} e^{-s\tau_1})(X_{22} - R_2 Y_{22} e^{-s\tau_2}) - (X_{12} - R_2 Y_{12} e^{-s\tau_2})(X_{21} - R_1 Y_{21} e^{-s\tau_1}) = 0. \quad (16)$$

This is achieved using Newton-Raphson iteration in the complex plane.

4.2 Evaluating the frequency response functions (FRFs)

The other piece of information we will require is the frequency response. This is given simply by setting $s = i\omega$ in Eq. (10).

4.3 Calculating the state-space matrices A, B, C, D

We want to be able to write the acoustic model described in § 2 in state-space form:

$$\dot{x}(t) = A\,x(t) + B\,q(t) \quad (17a)$$
$$y(t) = C\,x(t) + D\,q(t), \quad (17b)$$

where y is some output of interest. Taking Laplace transforms of Eq. (17) and rearranging, we arrive at the transfer function:

$$G(s) = \frac{y(s)}{q(s)} = C(sI - A)^{-1}B + D. \quad (18)$$

A state-space realization is not unique: that is, there are many state-space realizations that give the same transfer function. The form that is convenient for our purposes is a modal realization, where the A matrix is written as a diagonal matrix with its eigenvalues on its diagonal. For this realization, the term $(sI - A)^{-1}$ can be written simply as

$$(sI - A)^{-1} = \begin{bmatrix} s - \lambda_1 & \cdots & 0 \\ \vdots & \ddots & \vdots \\ 0 & \cdots & s - \lambda_n \end{bmatrix}^{-1} = \begin{bmatrix} \frac{1}{s-\lambda_1} & \cdots & 0 \\ \vdots & \ddots & \vdots \\ 0 & \cdots & \frac{1}{s-\lambda_n}. \end{bmatrix} \quad (19)$$

and the transfer function, $G(s)$, becomes

$$G(s) = \sum_{i=1}^{n} \frac{c_i b_i}{s - \lambda_i} = \sum_{i=1}^{n} \frac{\theta_i}{s - \lambda_i}. \tag{20}$$

This is for the single-input single-output case where B is a column vector and C is a row vector, but is easily extended to the multi-input multi-output case. Here we have defined $\theta_i = c_i b_i$. Now if we evaluate the frequency response of $G(s) = G(i\omega)$ at the frequencies $\omega_1, \omega_2, \ldots, \omega_p$, then we have

$$\begin{bmatrix} G(i\omega_1) \\ \vdots \\ G(i\omega_p) \end{bmatrix} = \begin{bmatrix} (i\omega_1 - \lambda_1)^{-1} & \cdots & (i\omega_1 - \lambda_n)^{-1} \\ \vdots & \ddots & \vdots \\ (i\omega_p - \lambda_1)^{-1} & \cdots & (i\omega_p - \lambda_n)^{-1} \end{bmatrix} \begin{bmatrix} \theta_1 \\ \vdots \\ \theta_n \end{bmatrix}, \tag{21}$$

which we can solve for $\begin{bmatrix}\theta_1 \ldots \theta_n\end{bmatrix}^T$. We need the frequency response at $p = n$ frequencies to make the matrix in Eq. (21) invertible. In practice, though, it is better to evaluate the frequency response at many more than n frequencies, $p \gg n$ and then solve Eq. (21) in the least squares sense. Notice that we have solved for $\theta_i = c_i b_i$. We are then free to choose any c_i, b_i, provided they satisfy $c_i b_i = \theta_i$.

4.4 Practical implementation

Clearly there is a frequency associated with each of the eigenvalues, $\lambda_1, \ldots, \lambda_n$, found by solving Eq. (16). We must bear these frequencies in mind when choosing the frequency range over which to evaluate the frequency responses, $G(i\omega)$, in Eq. (21). We can anticipate two scenarios that would cause a problem when solving Eq. (21):

- The maximum frequency used for the frequency response is *higher* than the frequency of the highest eigenvalue found. In this case, Eq. (21) will encounter modes in the frequency response that it does not know about.
- The maximum frequency used for the frequency response is *lower* than the frequency of the highest eigenvalue found. In this case, Eq. (21) will have some extra eigenvalues at high frequencies to play with, but the behaviour of these eigenvalues will not be constrained as it should be by the frequency response.

So by consistent, we mean that the maximum frequency used in the frequency response makes sense in relation to the frequency of the highest eigenvalue found.

5. Results

We now apply the method to the geometry shown in figure 1. The duct is 1 m long, and the heat release occurs 0.3 m from the upstream end. Therefore the values of l_1 and l_2 (refer to figure 1) are $l_1 = 0.3$ and $l_2 = 0.7$. For brevity we plot data at just one point in the duct, and the location chosen is $x = 0.4$. (Recall that x is measured from the flame.) Pressures are non-dimensionalized using $\gamma\overline{M_1 p_1}$, velocities are non-dimensionalized using $\overline{u_1}$, and the unsteady heat release is non-dimensionalized using $\overline{q}$. Time and frequency, meanwhile, remain dimensional.

The purpose of this section is to investigate how well the acoustics are captured by the state-space model. This is done in two ways: i) in the frequency domain by comparing the frequency response of the state-space model to that given directly by equations (10); and ii) in the time domain by comparing the state-space model's impulse response (for a Gaussian pulse) to that given by time-stepping the governing equations (8) directly. Notice in particular that we do not couple the acoustics to a flame model. Instead, the perturbation in the heat release rate is provided as an input (a Gaussian pulse) when we simulate the systems in the time domain. (Of course, coupling the acoustic state-space model to a suitable flame model is one of the ultimate aims of the model, but this is not required in order to *validate* it, which is what we are concerned with here.)

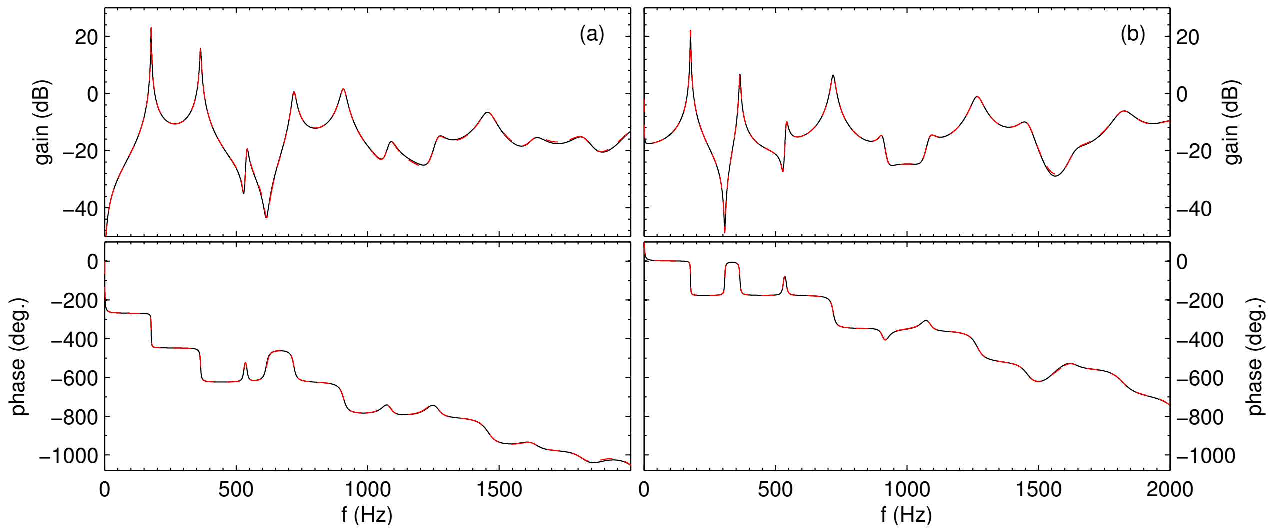

Figure 2. Comparison of the frequency responses found directly using Eq. (10) (——) and using the state-space model (– –) for (*a*) the pressure; and (*b*) the velocity. Both plots are for the location $x = 0.4$.

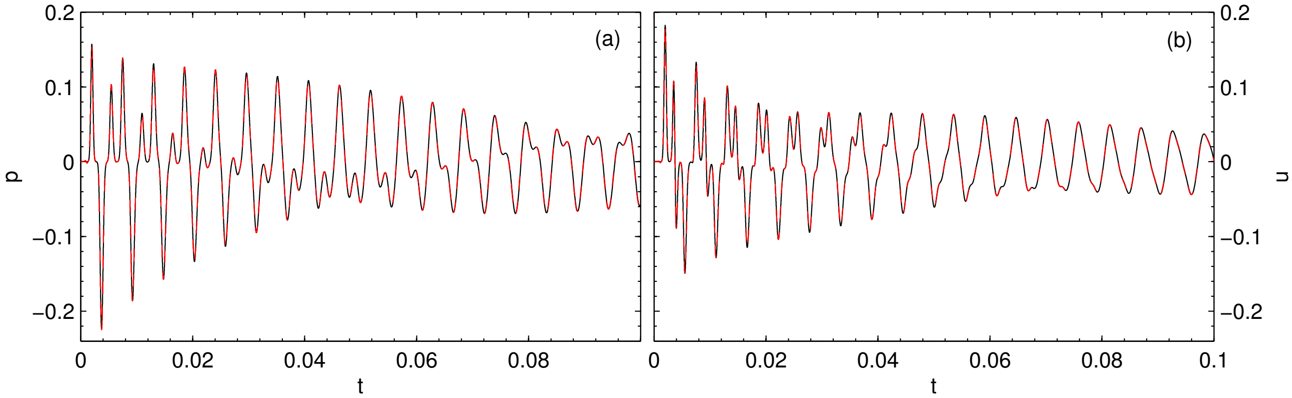

Figure 3. Comparison of the impulse responses found directly by time-stepping Eq. (8) (——) and using the state-space model (– –) for (*a*) the pressure; and (*b*) the velocity. Both plots are for the location $x = 0.4$.

5.1 Validation in the frequency domain

Figure 2 compares the frequency response of the state-space model, which is found by setting $s = i\omega$ in Eq. (18), to that found directly by evaluating Eq. (10). The agreement is excellent for both the pressure and the velocity. (There are some very small discrepancies at the highest frequencies shown, and this makes sense, since this is the frequency range in which the higher modes that have been discarded will have their greatest effect.) Similar agreement is seen at other locations in the duct.

5.2 Validation in the time domain

Figure 3 compares the response of the state-space model to that found directly by time-stepping Eq. (8) for a Gaussian impulse of the form: $q'(t)/Q = \exp\{-(t-t_0)^2/\sigma^2\}$, with $t_0 = 0.001$ s and $\sigma = 2.6904 \times 10^{-4}$. We see excellent agreement, with the pressure and velocity both very well-captured by the state-space model. Similar agreement is seen at other locations in the duct.

6. Conclusions

A method has been presented for finding a state-space description of an acoustic model when that model comes from a wave-based analysis. The method uses knowledge of the acoustic modes, together with the frequency response, to find the state-space description. This state-space description is very useful because it allows powerful, well-established tools from dynamics and control to be applied to the thermoacoustic system. The method has been demonstrated on a simple open-ended duct with a temperature jump across the flame, and good results are seen. The state-space model shows excellent agreement with the original model, both in the time domain and in the frequency domain. The method is sufficiently general that it can be applied to more complex configurations. The next step is to apply the method to a more complex geometry using data generated from a thermoacoustic network model. This will allow acoustic state-space models to be generated for combustors with both longitudinal and annular geometries.

A. X and Y matrices

The expressions for the X and Y matrices introduced in Eq. (6) are

$$X = \begin{bmatrix} -1 + \bar{M}_1(2 - \frac{\bar{u}_2}{\bar{u}_1}) - \bar{M}_1^2(1 - \frac{\bar{u}_2}{\bar{u}_1}) & +1 + \bar{M}_2 \\ \frac{1-\gamma\bar{M}_1}{\gamma-1} + \bar{M}_1^2 - \frac{1}{2}\bar{M}_1^2(1 - \bar{M}_1)(\frac{\bar{u}_2^2}{\bar{u}_1^2} - 1) & \frac{\bar{c}_2}{\bar{c}_1}\left(\frac{1+\gamma\bar{M}_2}{\gamma-1} + \bar{M}_2^2\right) \end{bmatrix}$$

$$Y = \begin{bmatrix} +1 + \bar{M}_1(2 - \frac{\bar{u}_2}{\bar{u}_1}) + \bar{M}_1^2(1 - \frac{\bar{u}_2}{\bar{u}_1}) & -1 + \bar{M}_2 \\ \frac{1+\gamma\bar{M}_1}{\gamma-1} + \bar{M}_1^2 - \frac{1}{2}\bar{M}_1^2(1 - \bar{M}_1)(\frac{\bar{u}_2^2}{\bar{u}_1^2} - 1) & \frac{\bar{c}_2}{\bar{c}_1}\left(\frac{1-\gamma\bar{M}_2}{\gamma-1} + \bar{M}_2^2\right) \end{bmatrix}.$$

References

[1] F. E. C. Culick, Nonlinear behavior of acoustic waves in combustion chambers—I, Acta Astronaut. 3 (1976) 715–734.

[2] F. E. C. Culick, Nonlinear behavior of acoustic waves in combustion chambers—II, Acta Astronaut. 3 (1976) 735–757.

[3] B. T. T. Zinn, M. E. Lores, Application of the Galerkin method in the solution of non-linear axial combustion instability problems in liquid rockets, Combust. Sci. Technol. 4 (1) (1971) 269–278.

[4] M. A. Heckl, M. S. Howe, Stability analysis of the Rijke tube with a Green's function approach, J. Sound Vib. 305 (4) (2007) 672–688.

[5] B. Schuermans, Modeling and control of thermoacoustic instabilities, Ph.D. thesis, Ecole Polytechnique Fédérale de Lausanne, 2003.

[6] S. Evesque, A. P. Dowling, A. M. Annaswamy, Self-tuning regulators for combustion oscillations, Proc. R. Soc. A 459 (2035) (2003) 1709–1749.

[7] A. P. Dowling, A. S. Morgans, Feedback control of combustion oscillations, Annu. Rev. Fluid Mech. 37 (2005) 151–182.

[8] S. R. Stow, A. P. Dowling, A Time-Domain Network Model for Nonlinear Thermoacoustic Oscillations, J. Eng. Gas Turbines Power 131 (3).

[9] A. P. Dowling, Nonlinear self-excited oscillations of a ducted flame, J. Fluid Mech. 346 (1997) 271–290.